Journal of the Korean Nuclear Society
Volume 32, Number 5, pp.446~456, October, 2000

The Application of a Laser to the Chemical Characterization of Radionuclides

Y. J. Park, K. K. Park, M. Y. Suh, S. K. Yoon, Y. S. Park, D. Y. Kim, and W. H. Kim

Korea Atomic Energy Research Institute
150 Dukjin-dong, Yusong-gu, Taejon 305-353, Korea
nyjpark@kaeri.re.kr

(Received October 29, 1999)

Abstract

Laser induced photoacoustic, fluorescence, and photon correlation spectroscopies were applied to the chemical characterization of radionuclides in connection with the radiowaste treatment and disposal. Their measuring principles and systems were briefly described together with their advantages over conventional spectroscopies. Also, other applications of lasers are introduced. Laser induced photoacoustic spectra were measured for a Pr^{3+} solution with a very low molar absorptivity. The detection sensitivity was 4.3×10^{-5} cm^{-1} and was 100 times better than that of a UV/VIS spectrophotometer. The Eu(III) excitation spectra($^7F_0 \rightarrow {}^5D_0$ transition) were measured for Eu(III)-phthalate complexes using laser fluorescence spectroscopy, showing that only two species, 1:1 and 1:2 complexes, are present in the Eu(III)-phthalic acid system. The size and size distribution for colloidal humic acids and Eu(III)-humate colloids was determined using photon correlation spectroscopy. The presence of Eu(III) enhanced the aggregation of humic acids.

Key Words : photoacoustic, fluorescence, photon correlation spectroscopies, speciation, colloid

1. Introduction

Solubilities, sorption phenomena occurring at the water-solid interface, and the colloid formation by humic substances have been studied for a better understanding of radionuclides' migration behaviors in groundwater in relation to the radiowaste disposal. For these purposes, a speciation of the chemical state of radionuclides in given groundwater conditions is an essential prerequisit. Since radionuclides normally exist in a very low concentration level in groundwater, a non-destructive speciation method of high sensitivity is required. Recently, several highly sensitive spectroscopic methods have been developed, based on a powerful laser light source,

and applied to the speciation of aquatic radionuclides in the submicromolar concentration range. In the present paper, three laser spectroscopic methods, laser induced photoacoustic spectroscopy (LPAS), laser induced fluorescence spectroscopy (LIFS), and photon correlation spectroscopy (PCS) are introduced, together with their measuring principles, system set-ups, and the results obtained from these methods.

1.1. LPAS

1.1.1. Measuring Principle

The molecules and atoms in the sample solutions are excited when they are illuminated with laser beams and then thermally deactivated to lower energy levels. The induced heat causes the sample section illuminated to expand. When a chopped light is used, the periodic expansion and contraction of the sample volume is generated, creating pressure waves (acoustic signals) which are detected by a piezoelectric transducer. Since the photoacoustic signals are due to light absorption by the sample, the photoacoustic spectrum is similar to that measured from a conventional UV/Visible absorption spectrophotometer. LPAS has an advantage over conventional absorption spectroscopy. While the former measures the signals proportional to an absolute light absorption, the latter does the signals depending on the ratio of transmitted and incident light intensities. Therefore, an increase in light power conspicuously enhances the photoacoustic signals, but gives little effect on the UV/Visible absorption signals. Since LPAS is much more sensitive than conventional absorption spectroscopies, it has been used for chemical speciation and the determination of concentration in a very low concentration range.

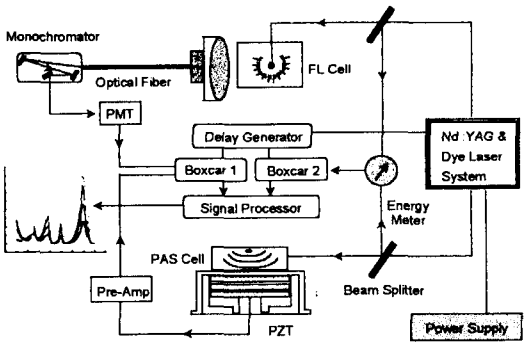

Fig. 1. Schematic Diagram of Laser Induced Photoacoustic Spectroscopy

1.1.2. Experimental Setup

A schematic diagram of the system used in LPAS is shown in Fig. 1. A pulsed Nd:YAG pumped dye laser (Spectron Laser Systems, SL-805G & SL-4000B) is used as the light source. The laser beams passing through a beam splitter are directed to the sample cell. The photoacoustic signals generated in the sample are detected by a piezoelectric transducer, converted to piezoelectric signals, amplified by a preamplifier (Stanford Research Systems, SR560), and finally fed into the channel of boxcar 2 (EG & G PARC, Model 4420). The pulse energy of the laser beams partially reflected (ca. 10 %) by the beam splitter is measured by an energy meter (Gentec, ED-200) and fed into the channel of boxcar 1. Boxcars 1 and 2 are synchronized by a delay generator (Stanford Research Systems, DG 535) to measure pulse energies and photoacoustic signals simultaneously. The signals measured in the two boxcars are fed into a signal processor(EG & G PARC, Model 4420) to obtain the normalized photoacoustic spectra.

1.1.3. Application

LPAS is applicable to gaseous, liquid, and solid

samples. It has strong advantages over conventional absorption spectroscopy for opaque and transparent samples. LPAS has been used particularly for the determination of trace amounts of samples and chemical speciation because of its high detection sensitivity and its real time response. It has been applied to the speciation of aquatic actinide ions [1-4] and to various speciation studies [5, 6] in association with the migration of actinides in natural aquifer systems[7]. In addition, LPAS can be used to great advantage in the study of adsorbed and chemisorbed molecular species and compounds on the surface of metals, semiconductors, and even insulators [8-10], and in the study of biological systems [11, 12] and medicine [13-15]. The application of LPAS has been extended to determine the thermal diffusivity and the thermal conductivity which are very important in heat-flow studies [16], and to the depth-profiling and thickness measurements of samples [17].

1.2. LIFS

1.2.1. Measuring Principle

The molecules and atoms in sample solutions absorb the laser beams to be excited when they are illuminated, and then deactivated to lower energy levels to produce emission lines. A simultaneous determination of wavelength and lifetime of fluorescence provides two dimensional information on the electronic structure of fluorescing ions. Therefore, LIFS is expected to yield more specific information than absorption spectroscopy and hence to increase the speciation capability in solution. While LIFS is applicable to analize the trace sample because of its high detection sensitivity, its use is limited to only fluorescent samples. In this study, Eu(III) excitation spectroscopy involving the $^7F_0 \rightarrow {}^5D_0$ transition was used as a luminescence probe of metal-ligand complexations. The $^7F_0 \rightarrow {}^5D_0$ transition is unique in that both the ground and the excited states are nondegenerate, and the levels of these states are not split by the crystal field exerted by ligands. Therefore, each peak may be considered as representing one individual Eu(III) species, thereby making this method suitable for the study of Eu(III)-ligand complexation.

1.2.2. Experimental Setup

The LIFS system shares with the light source and the measuring devices of LPAS, and is additionally equipped with the detection assembly as shown in Fig. 1. The fluorescences emitting from the sample cell are collected into the optical fiber and directed to a monochromator. The only fluorescence intended to be measure enters the photomultiplier tube and then its electrical signal is fed into the boxcar integrator. The remaining procedures are the same as in the LPAS system. A combination of LPAS and LIFS provides a powerful spectroscopic speciation method that can give a new dimension of high reliability to the study of actinide migration. For this study, the second harmonics of the Nd:YAG laser was used to pump a rhodamine 590 and 610 dye mixture with spectral range 573-593 nm. The bandwidth of the dye laser was 1.0 cm^{-1}(0.03 nm), the laser pulse width was 10 ns, and the pulse energy was kept just below 5 mJ. The fluorescence (616 nm) originating from the $^5D_0 \rightarrow {}^7F_2$ transition was detected by PMT (DA-20, Attago Bussan Co.) followed by dc amplification. The Eu(III) excitation spectra ($^7F_0 \rightarrow {}^5D_0$ transition) were acquired in the ratio mode using two boxcar averagers and a signal processor. To obtain each spectrum with an enhanced S/N ratio, five spectra were acquired and averaged. The signal processor was GPIB-interfaced to an IBM-PC/AT, and all the data

were transferred and analyzed with PeakFit software (Version 4.02, Jandel Co.). Eu(III) excitation spectra were deconvoluted using a nonlinear least-squares routine: The sum of several peaks having a Lorentzian-Gaussian function, I exp {-2 [(x - *W*) / *L*)^2} / {2 [(x - *W*) / L]^2 + 1}, where *I*, *W*, and *L* are the intensity, peak position, and linewidth, respectively.

1.2.3. Application

LIFS has been frequently used for the studies of chemical speciation and for the determination of trace amounts of the sample in aqueous solutions because of its high detection sensitivity. Since many of organic compounds can emit fluorescences, LIFS is a powerful tool to analyze them. However, there are not many metals emitting fluorescences. The fluorescent metals of radionuclides using this technique are Cm(III) [18], U(VI) [19], and lanthanide ions [18].

1.3. PCS

1.3.1. Measuring Principle

The PCS method consists of determining the velocity distribution of particles movement by measuring the dynamic fluctuations in the intensity of scattered light. The colloidal particles present in aqueous solutions undergo Brownian motion which causes the fluctuations in the local concentration of particles, resulting in local inhomogeneities of the refractive index. This in turn results in the intensity fluctuations of the scattered light. The linewidth of the light scattered spectrum Γ (defined as the half-width at half-maximum) is proportional to the diffusion coefficient of the particles (D): $\Gamma = Dk^2$, where $k = (4\pi n/\lambda)\sin(\theta/2)$; n is the refractive index of the medium, λ the laser wavelength, and θ the scattering angle. With the assumption that the particles are spherical and non-interacting, the mean radius is obtained from the Stokes-Einstein equation: $r = k_B T / 6\pi\eta D$, where k_B is the Boltzman constant, T is temperature, and η is the shear viscosity of the solvent. Information about the light-scattering spectrum can be obtained from the autocorrelation function G(t) of the light-scattering intensity: G(t) = A exp(-Γt) + B. The characteristic decay time of the correlation function is inversly proportional to the linewidth of the spectrum. Therefore, the diffusion coefficient and particle size can be determined by fitting the measured correlation function to a single exponential function.

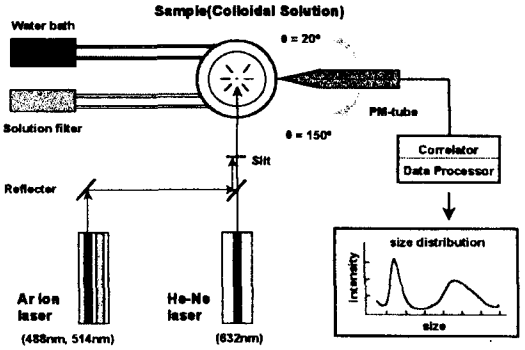

Fig. 2. Schematic Diagram Photon Correlation Spectroscopy

1.3.2. Experimental Setup

A schematic layout of PCS (Brookhaven Instrument Co., Model BI-9000) is shown in Fig. 2. A He-Ne laser (632.8 ㎚, 35 mW) or Ar ion laser (488 nm, 514 nm) is used as the light source. A pyrex glass cylindrical cell (10 mm) containing the sample is maintained to be at a constant temperature with a circulating water bath. The scattered light from the cell is detected at a given angle by a photomultiplier tube (PMT), and the

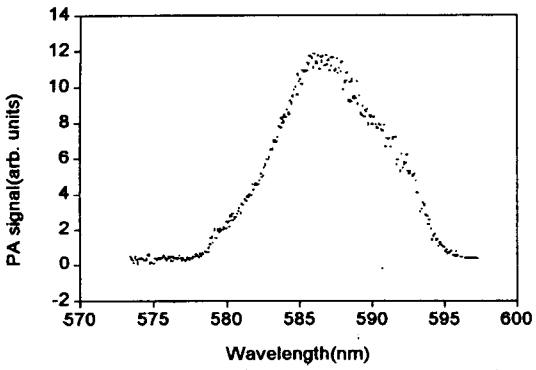

Fig. 3. PA Spectrum of Pr^{3+}ion in Aqueous Solution

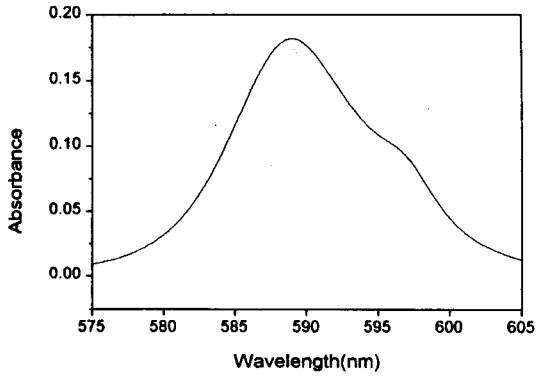

Fig. 4. UV/VIS Absorption Spectrum of Pr^{3+} Solution

measured signal is fed into a correlator. The size and the size distribution of the sample are determined by data processing. The Ar ion laser is used for the small colloids present in low concentrations since its wavength is relatively shorter and the energy is higher than the He-Ne laser. In this study, the He-Ne laser was used for humic acids of large sizes and relatively high concentrations.

1.3.3. Application

PCS can be used to determine the size and the size distribution of the particles with their size ranging from 10 to 1000 nm and also the molecular weight of the particles (> 10^5 Dalton). The PCS system used in this study can detect particles of 5 - 3000 nm. In connection with the radiowaste disposal, interactions with radionuclides and humic acids play an important role in the migration of radionuclides. The data of the size and distribution of humic acids and colloidal metal-humic acids provide much useful information on aggregation and dissociation phenomena, stability of colloids, and structure of colloids [20].

2. Results and Discussion

2.1. LPAS

A Pr^{3+} stock solution was prepared by dissolving Pr_6O_{11} (99.9 %, Aldrich Chem. Co.) in doubly distilled water with the least addition of concentrated $HClO_4$ solutions. The Pr^{3+} sample solutions were prepared by diluting the stock solution. The photoacoustic spectrum of 0.02 M Pr^{3+} ion was obtained in the yellow region (570 - 600 nm). As shown in Fig. 3, the absorption peak maximum at 588.8 nm is known to be due to the transition of the ground state $^3H_4$ to the excited state $^1D_2$. Fig. 4 shows the absorption spectrum of the 0.1 M Pr^{3+}solution. From Figs. 3 and 4, it can be seen that the absorption maxima of these two spectra appear at the same wavelength (588.8 nm) and the shapes are almost the same. Generally, in the near UV-Visible region, the molar absorptivities for the absorption band maxima of all trivalent lanthanides are weak and subsequently these elements are difficult to analyze with classical spectroscopic methods [21]. The molar

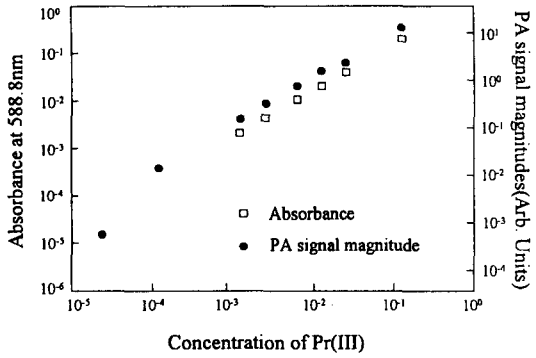

Fig. 5. Correlation of Photoacoustic Signal and Absorbances with Concentration of Pr^{3+}ion in Aqueous Solution

absorptivity of the 0.1 M Pr^{3+} solution at 588.8 nm was found to be 1.6 $M^{-1}cm^{-1}$. This implies that a slight variation in absorptivity at a large transmission is extremely difficult to detect by absorption spectrometry. On the other hand, LPAS can detect a change of an absorptivity of 10^{-5} cm^{-1}[22]. The comparative study on the detectability of LPAS and absorption spectrometry was carried out using aqueous solutions containing Pr^{3+} ions in different concentrations from 1.2×10^{-1} to 2.7×10^{-5} M. The maximum intensities measured at 588.8 nm are plotted against Pr^{3+} concentration in Fig. 5, showing that the intensity is linearly proportional to the aquo Pr^{3+} ion concentration in the two cases. The absorbances below 1.2×10^{-3} M could not be measured by absorption spectrometry whereas the photoacoustic signals could be detected down to 2.7×10^{-5} M by LPAS. The absorptivity detectable by absorption spectrometry was found to be at most 2×10^{-3} cm^{-1}, whereas the minimal absorptivity detectable by LPAS was found to be 4.3×10^{-5} cm^{-1} at 588.8 nm. This indicates that LPAS is about 100 times more sensitive than UV/VIS. The

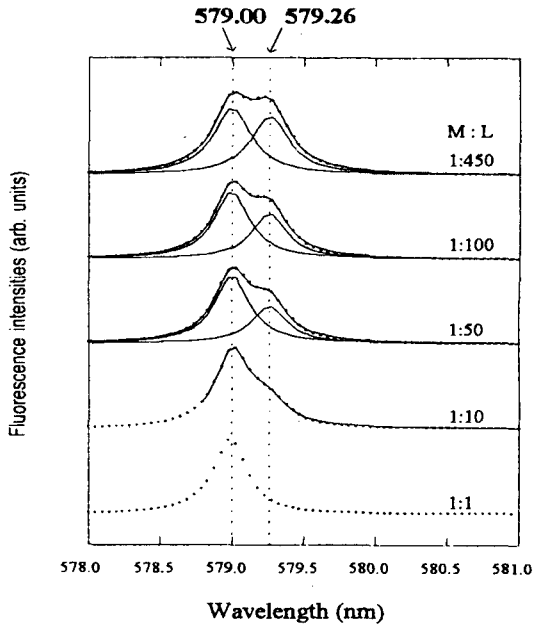

Fig. 6. Deconvoluted Excitation Spectra of Eu(III)-Phthalic Acid Systems with a Variation of Ligand Concentration

average accuracy obtained with our LPAS was about 3%. A better accuracy may be obtained statistically by multiscanning to improve the signal-to-noise ratio. In the case that this LPAS system is applied to Am^{3+} solutions, it is expected to detect the minimum concentration of 2×10^{-5} M (ε= 400 M^{-1} cm^{-1} at 503 nm) when the absorbance of water is about 2.6×10^{-4} cm^{-1} at 503 nm. From this detection sensitivity and accuracy, LPAS can be used for the speciation and determination of the concentration of radionuclide ions in trace levels.

2.2. LIFS

The Eu(III) solution was prepared by dissolving $EuCl_3 \cdot 6H_2O$ (99.99% Aldrich Co.) in doubly deionized water. Phthalic acid used as on organic ligand was of reagent grade or better and was

used without further purification. The series of sample solutions were prepared by mixing appropriate amounts of Eu(III) and phthalic acid solutions at 25℃ . Typically the Eu(III) concentration was kept constant at 1.0×10^{-3} M and the concentration of the ligand was varied from 1.0×10^{-3} to 4.5×10^{-1} M. The sample solutions were kept overnight to equilibrate. The pH of the solution was adjusted with 0.1 M HCl and 0.1 M NaOH (carbonated free, Baker Co.), and checked prior to spectral analysis with a glass electrode coupled to a digital pH meter (Metrohm Type 632). The Eu(III) excitation spectra for the Eu(III)-phthalic acid system were obtained in aqueous solution. Fig. 6 shows the series of spectra obtained by varying the ligand-to-metal concentration ratio from 1 to 450 while keeping the pH constant at 6.0. As a consequence of the peak deconvolution, two identifiable peaks appeared at 579.00 and 579.26 nm suggesting the formation of two different Eu(III)-phthalate complexes in aqueous solutions with increasing phthalic acid concentrations. The 1:1 complex (EuL^{2+}) and 1:2 complex (EuL_2^{+}), where L represents a ligand molecule, correspond to the peaks at 579.00 and 579.26 nm, respectively. The peak positions and the number of peaks obtained inr the Eu(III)-phthalic acid system were almost the same as in the Eu(III)-acetic acid system. Since acetic acid has one carboxylate group, the 1:2 complexes are formed through the binding of the two molecules to Eu(III) ions. Phthalic acid contains two carbolxylate groups in the moiety. If the two carboxylate groups of phthalic acid are bound to the Eu(III) ions simultaneously and the 1:1 complexes are formed, the peak position is to be quite different from that of the 1:2 Eu(III)-acetate complexes. The experimental results show that this is not the case. In the case that one molecule of phthalic acid binds bidentately to the Eu(III) ions through the two carboxylate groups, a very unstable seven-membered ring will be formed. This is not acceptable from the viewpoint of thermodynamics. Therefore, it is confirmed that the 1:2 Eu(III)-phthalate complexes originate from the binding of two molecules of phthalic acid. This was also supported by measurements of the number of water molecules coordinated to the Eu(III) ions [23, 24].

2.3. PCS

A Eu(III) stock solution was prepared from the following procedure: An exact amount of $Eu(NO_3)_3\cdot5H_2O$ was weighed, dissolved in doubly deionized water, heated several times, and finally $Eu(OH)_3$ free of nitrate was obtained. A 1.00×10^{-2} M Eu(III) stock solution was prepared from the dissolution of $Eu(OH_3)$ in the 0.1M $NaClO_4$ solutions containing 5.0×10^{-4}M 4-morpho-lineethane sulfonic acid (MES). To prepare the humic acid stock solution, humic acid (Aldrich Chem. Co.) was purified using the precipitation method in acid and base solutions and then the H^+-type humic acids were obtained. A weighed amount (0.0201 g) of the H^+-humic acid was dissolved in 1 mL of 0.1 M NaOH and then the buffer solutions (0.1 M $NaClO_4$/5.0 × 10^{-4} M MES, pH = 6.0) were added, and finally a humic acid stock solution of 200 ppm was prepered.

2.3.1. Measurement of the Size and Size Distribution of the Humic Acid

Two humic acid samples of 20 and 100 ppm were prepared by diluting the stock solution with 0.1M $NaClO_4$/5.0×10^{-4} M MES solutions. Each sample solution was filtrated using filters with sizes of 220 and 450 nm. The scattered light intensities for the samples were measured at

Table 1. Measured Hydrodynamic Radius(R_h) of Humic Acids After Filtrating with 220nm and 450nm Pore Size Filters

pore size (nm)	concentration (ppm)	Diffusion Coefficient($\times 10^8$) Angle 45°	60°	75°	90°	R_h[(a)]
450	100	1.982	2.098	2.282	2.463	274.8nm
	20	2.222	2.331	2.421	2.542	231.3nm
220	100	3.549	3.626	3.767	3.914	145.0nm
	20	5.328	5.572	5.791	5.969	96.2nm

(a) correlation coefficients (r) > 0.990

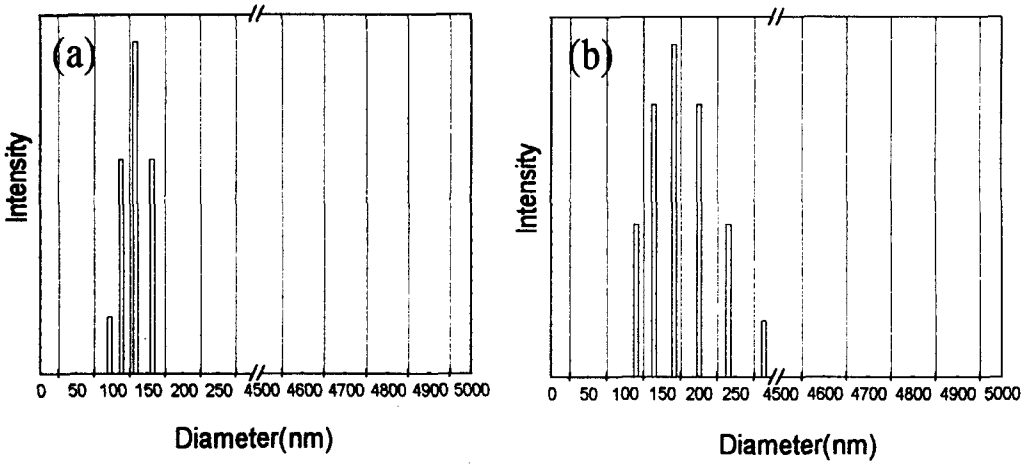

Fig. 7. The Size Distributions of Humic Acids at 100 ppm Concentration. The Humic Acid was Filtrated with 220 (a) and 450 nm(b) Pore Size Filter. The Scattered Light Intensity was Measured at a Right Angle

angles of 45, 60, 75, and 90 degrees before and after filtration. For the unfiltrated samples, reliable data were not obtained because of the significant fluctuations. The data for the filtrated samples are listed in Table 1, which shows the diffusion coefficients obtained from the fluctuations of the scattered light intensity and hydrodynamic radius(R_h) calculated from the Stokes-Einstein equation. It can be seen that the hydrodynamic radius of the colloidal humic acids was larger for the higher concentration. This suggests that the aggregation of humic acids occurs by van der Waals interactions as the concentration increases. The effect of the concentration on size will be described in detail later. The size distribution of humic acids (100 ppm) filtrated using filters of 220 and 450 nm was determined from the scattered light intensities measured at a right angle and shown in Fig. 7. The sizes exhibiting the maximum distributions were 133 and 166 nm for the filtrations with pore sizes of 220 and 450 nm,

Table 2. Measured Hydrodynamic Diameter, R_h, of Humic Acid in the Presence of Eu(III) ion at Various Passing Time. Humic Acid Concentration is 40ppm. The Scattered Light Intensity was Measured at a Right Angle

$[Eu(III)]_{tot}$	passed time(day)			
$\times 10^6$, M	0	1	6	21
1.0	71 ± 2 447 ± 25	71 ± 4 419 ± 46	81 ± 4 375 ± 106	81 ± 3 261 ± 22
5.0	84 ± 13 478 ± 131	86 ± 18 452 ± 113	77 ± 4 240 ± 35	67 ± 11 202 ± 48
8.0	96 ± 15 743 ± 209	84 ± 14 603 ± 221	80 ± 2 411 ± 17	64 ± 12 186 ± 39

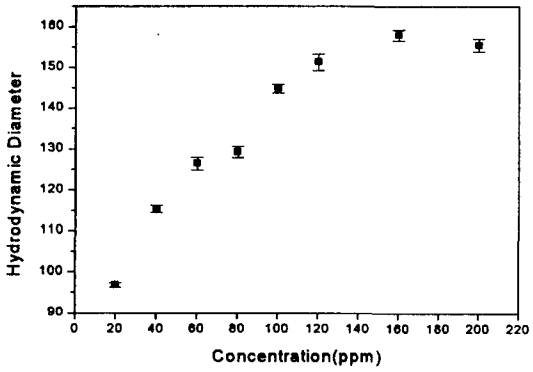

Fig. 8. The Plot of Measured Hydrodynamic Diameter (R_h) of Humic Acid as a Function of Humic Acid Concentration

respectively. It can be seen that the sizes for the sample filtrated with the smaller pore size are distributed over a narrower range. Therefore, the use of 220 nm-filter is favorable to measure changes in the size distribution by the interaction between metal ions and humic acids.

2.3.2. Effect of Concentration on Size Distributions

A series of humic acid solutions were prepared from the stock solution. The concentrations of the samples were 20, 40, 60, 80, 100, 120, 160, and 200 ppm and were filtrated using 220 nm-filters. The scattered light intensities for each sample were measured at angles of 45, 60, 75, and 90 degrees. The hydrodynamic radius(R_h) is plotted against the concentration in Fig. 8. The R_h increased as the concentration increased up to 160 ppm and then reached a plateau. Humic acid is a polyelectrolytic macromolecule and contains a number of molecules with different molecular weights and structures in it. The electrical charge of the molecule with a circle structure is delocalized all over the molecule. On the other hand, the electrical charge of the molecule with a straight structure is localized and thus the molecules aggregate as the concentration increases. The observation that the size does not increase above 160 ppm indicates that the aggregation is saturated.

2.3.3. Effect of Metal ions on the Size of Humic Acids

The presence of Eu(III) is expected to accelerate the aggregation of humic acids and thus the concentration of humic acid used was lowered to 40 ppm. The concentration of Eu(III) was 1.0×10^{-6}, 5.0×10^{-6}, and 8.0×10^{-6}M. The scattered light intensities for the samples were measured at a right angle at appropriate time

intervals. The measurement for each sample was carried out seven times or more. The results are listed in Table 2. Two types of colloids with different sizes were observed. It is expected that the larger colloids are associated more with Eu(Ⅲ) ions than the smaller colloids. As the concentration of Eu(Ⅲ) was higher, the sizes of the colloids were larger. This implies that the interaction between Eu(Ⅲ) and humic acids enhances the aggregation of humic acids. The larger colloid became smaller and smaller irrespective of Eu(Ⅲ) concentration as time passed. This indicates that the complexes formed between Eu(Ⅲ) ions and humic acids rearrange slowly to reduce the size or the precipitation occurs invisibly. The size of the smaller colloids was not significantly changed with time, compared to the larger colloids. This means that the smaller colloids are not greatly associated with Eu(Ⅲ) ions.

3. Conclusions

Three spectroscopic techniques using a laser, LPAS, LIFS and PCS can be used to study chemical speciation and colloid formation, and to determine the concentration of radionuclides in trace levels. Especially, they are very useful for studies on the migration of radionuclides in groudwater.

Acknowledgment

This work was carried out under the Nuclear R & D Program by the Ministry of Science and Technology.

References

1. W. Schrepp, R. Stumpe, J. I. Kim, H. Walther, *Appl. Phys.* **B32**, 207 (1983).
2. R. Stumpe, J .I. Kim, W. Schrepp, and H. Walther, *Appl. Phys.* **B34**, 203 (1984).
3. S. Okajima, D. T. Reed, J. V. Beitz, C. A. Sabau, and D. L. Bowers, *Radiochim. Acta.* **52/53**, 111 (1991).
4. R. Klenze, J. I. Kim, and H. Wimmer, *Radiochim. Acta.* **52/53**, 97 (1991).
5. S. Magirius, W. T. Carnell, and J. I. Kim, *Radiochim. Acta* **38**, 29 (1985).
6. M. Eiswirth, J. I. Kim, and Ch. Lierse, *Radiochim. Acta* **38**, 197 (1985).
7. J. I. Kim, W. Treiber, Ch, Lierse, and P. Offermann, *Mat. Res. Soc. Symp. Proc.* **44**, 359 (1985).
8. A. Rosencwaig, and S. S. Hall, *Anal. Chem.*, **47**, 548 (1975).
9. M. J. Low, and G. A. Parodi, Spectrosc. Lett., 11, 581 (1978).
10. A. J. Maeland, R. Rittenhaus, W. Lahar, and P. V. Romano, *Thin Solid Films*, **21**, 67 (1974).
11. S. W. Jeffrey, M. Sielicki, and F. T. Haxo, J. Phycol., 11, 374 (1975).
12. K. Sauer and R. Park, Biochim. *Biophys. Acta* **79**, 476 (1964).
13. S. D. Campbell, S. S. Yee, and M. A. Afromowitz, *J. Bioeng.* **1**, 185 (1977).
14. R. van Heyningen, *Sci. Am.* **233**, 70 (1975).
15. A. Rosencwaig, and E. Pines, *Biochem. Biophys. Acta.* **403**, 10 (1977).
16. Y. S. Touloukian, R. W. Powell, C. Y. Ho, and M. C. Nicolasu, *Thermal Diffusivity*, 1973, IFI/Pleum, New York.
17. M. J. Adams, and G. F. Kirkbright, Analyst, 102, 678 (1977).
18. C. Moulin, P. Decambox, L. Couston, and D. Pouyat, *J. Nucl. Sci. Technol.*, 31, 691 (1994).
19. N. Delorme, *Radiochim. Acta* **52/53**, 105 (1991).

20. van de Hulst, Light Scattering by Small Particles, Dover Publication Inc., New York, (1981).
21. W. Carnell, Handbook on the Physics and Chemistry of rare earths, edited by K. A. Gschneider, jr. and L. Eyring, Chapter 24 (1979).
22. T. Sawada, S. Oda, and H. Kamada, *Proc. Jpn. Acad. Ser.* B, 54, 189 (1978).
23. B. H. Lee, K. H. Chung, H. S. Shin, Y. J. Park, and H. Moon, *J. Colloid Interface Sci.*, **188**, 439 (1997).
24. Y. J. Park, B. H. Lee, W. H. Kim, and Y. K. Do, *J. Colloid Interface Sci.*, **209**, 268 (1999).